Detection of the time dependent gravity field and Global Change

R. Sabadini[1], G. Di Donato[1], L. L. A. Vermeersen[2], R. Devoti[3], V. Luceri[3], and G. Bianco[4]

[1] *Dipartimento di Scienze della Terra, Università di Milano, Italy.*

[2] *DEOS, Faculty of Aerospace Engineering, Delft University of Technology, Netherlands.*

[3] *Telespazio S.p.A., Centro di Geodesia Spaziale 'G . Colombo', Matera, Italy*

[4] *Agenzia Spaziale Italiana, Centro di Geodesia Spaziale 'G . Colombo', Matera, Italy*

Abstract. Long wavelength time variations of the gravity field detected by means of laser tracking of geodetic satellites provide nowadays the unique opportunity to infer simultaneously the lower mantle viscosity and the mass imbalance in the polar regions of the Earth. Present day mass instabilities in Antarctica and Greenland and the flow of mantle material following the Pleistocenic deglaciation are the sources of the long wavelength time variations of the gravity field. In the present analysis we explore the effects of postglacial rebound and ice loss in Antarctica and Greenland on the secular drift of the even and odd zonal components of the geopotential by means of viscoelatic stratified Earth models and our capability to infer the mantle viscosity and lithospheric thickness.

Introduction

Two major mechanisms are responsible for the secular changes in the gravitational field: the Pleistocenic deglaciation, that ended about seven thousands years ago, and the present day mass instability in Antarctica, Greenland and Alpine glaciers. The Earth is affected today by the first mechanism because of the viscous memory of the mantle and by the second due to ongoing surface mass redistribution.

Secular changes in the long wavelength gravitational field are accurately detected by means of laser tracking of geodetic satellites [*Cheng et al.*, 1997; *Devoti et al.*, 2001]. In the dynamical Satellite Laser Ranging data analysis approach the satellite orbit can be used as a gravity probe to monitor the time varying gravity field. A long history of SLR observations of the geodetic satellites LAGEOS-I, LAGEOS-II, Starlette and Stella have been analyzed by *Devoti et al.* [2001] in order to estimate the time series of the low degree zonal coefficients in the Earth gravity field, and derive their secular drifts, up to degree six. Comparison of these zonal rates with the results of the viscoelastic Earth models forced by Pleistocene deglaciation, shows that the SLR retrieved even and odd zonals can be used today to infer the mantle viscosity and the lithospheric thickness of the Earth.

Inference of mantle viscosity and lithospheric thickness

In *Devoti et al.* [2001] the observations of four geodetic satellites has been analysed covering the period 1987-1998, spanning 11 years of LAGEOS-1 and Starlette observations and respectively 5 and 4 years of LAGEOS-2 and Stella observations. Unmodeled and mismodeled tidal and non-gravitational perturbations could in principle affect the long term gravity signal and may partly explain the discrepancies between the time derivatives of the zonals given in Tables 1 and 2, taken from *Devoti et al.* [2001], and recent published results [*Cazenave et al.*, 1995; *Eanes*, 1995; *Nerem and Klosko*, 1995; *Cheng et al.*, 1997]. Another critical point in treating a long period of tracking data arises from the lack of homogeneity in the data quality and distribution. *Devoti et al.* [2001] provide a detailed description of the techniques that have been applied to recover the zonals.

In order to explore the capability of our SLR retrieved zonals to infer the mantle viscosity and the lithospheric thickness L, we model the viscoelastic response of our planet to Pleistocenic deglaciation, the major contributor to the zonal rates; the ice model is the ICE-3G by *Tushingham and Peltier* [1991]. In this section, present day forcing is not included in the modeling, and we thus assume that Pleistocenic deglaciation is the only forcing contributor. We can look for discrepancies in the results of the modelling as possible indicators for present day ice melt or growth. In Figure 1 and 2 a χ^2 analysis is carried out for each of the zonals of Tables 1 and 2 estimated by *Devoti et al.* [2001], in order to explore their preferred lower and upper mantle viscosities, ν_2 and ν_1 and lithospheric thickness, L, and to enlighten possible discrepancies among these best fit parameters. The χ^2 analysis for each zonal separately is given by

$$\chi^2 = \left(\frac{\dot{J}_l^{mod} - \dot{J}_l^{obs}}{\sigma_l^{obs}}\right)^2 \tag{1}$$

where $\dot{J}_{obs}$ and $\dot{J}_{mod}$ correspond to the zonal of the tables and that retrieved from the model respectively.

The regions where the χ^2 obtain their (local) minima give the best fit between observed and modeled values. In agreement with *Vermersen et al.* [1998] where, except for the odd one, the χ^2 analysis was carried out for all the zonals simultaneously or the zonal plus the true polar wander induced by the melting of the Pleistocene ice sheets, the best fit in Figure 1 falls in two main regions, one in which the lower mantle viscosity is high, of the order of 10^{23} Pa s, and another one in which it is of the order of 10^{21} Pa s or lower.

Figure 1 shows that the tendency of this multiplicity of solutions is a characteristic of each zonal. The best fit ν_2 varies among the zonals, with a clear tendency for $\dot{J}_{odd}$, $\dot{J}_4$ and $\dot{J}_6$ towards lower mantle viscosities that fall beyond the limits stated above, with $\nu_2 < 10^{21}$ Pa s and $\nu_2 > 10^{23}$ Pa s. On the contrary, the best fit lower mantle viscosity for $\dot{J}_2$ is 21.2 in the logarithmic scale. This discrepancy between $\dot{J}_2$ and the other zonals indicates that, beyond post-glacial rebound, another mechanism of mass redistribution must be active. Another interesting result of Figure 1 is that the best fit upper mantle viscosity is lower than 10^{21} Pa s, for $\nu_2 = 10^{21}$ Pa s; in particular, $\nu_1 = 10^{20.6}$ Pa s for $\dot{J}_2$. For the best fit corresponding to $\nu_2 > 10^{23}$ Pa s, it is interesting to note that the upper mantle viscosity should be higher than 10^{21} Pa s. These results indicate an upper mantle viscosity considerably lower than 10^{21} Pa s for a lower mantle viscosity of the order of $10^{21} - 10^{22}$ Pa s. in good agreement with previous findings [*Nakada and Lambeck*, 1989: *Forte and Mitrovica*, 1996]. The zonal analysis carried out in Figure 1 shows that the sensitivity to lower mantle viscosity variation is the highest for $\dot{J}_2$ and $\dot{J}_{odd}$, the lowest being for $\dot{J}_6$ and somehow intermediate for $\dot{J}_4$. The highest sensitivity to upper mantle viscosity variations is carried out by $\dot{J}_2$ for ν_2 of the order of 10^{21} Pa s, and by the other zonals for ν_2 of the order of 10^{23} Pa s.

The same χ^2 analysis is carried out in Figure 2 for the lithospheric thickness and the upper mantle viscosity. As observed in this figure, the preferred upper mantle viscosity is generally lower than 10^{21} Pa s. In particular, a local minimum in $\dot{J}_6$ corresponds to an upper mantle viscosity of 20.4 in logarithmic scale.

Consistently with $\dot{J}_6$, upper mantle viscosities lower than 20.6 are indicated by $\dot{J}_{odd}$. This tendency to upper mantle viscosities lower than 10^{21} Pa s is carried out also by $\dot{J}_2$ and $\dot{J}_4$, although the sensitivity to upper mantle viscosity variations is the lowest for $\dot{J}_4$. When we consider the best fit lithospheric thickness, it is remarkable that $\dot{J}_4$ and $\dot{J}_6$ are sensitive to lithospheric thickness variations, and indicate coherently a lithosphere of 80-100 km. This finding is in contrast with $\dot{J}_2$, where local minima indicate lithospheric thickness lower than 40 km or higher than 180 km. Also this discrepancy could be interpreted as an indication of ongoing mass redistribution over the Earth.

Some interesting observations can be done if we compare the viscosity values that allow to fit the various harmonics or we test the mutual consistency of the different SLR analyses of Tables 1 and 2. For an upper mantle viscosity of 10^{21} Pa s $\dot{J}_2$ can be fitted by a lower mantle viscosity of 1.5×10^{21} Pa s, while $\dot{J}_{odd}$ resulting from this study or from *Cheng et al.* [1997] requires a lower mantle viscosity of $2 - 6 \times 10^{20}$ Pa s; the datum of *Nerem and Klosko* [1995] for $\dot{J}_{odd}$ requires 1.0×10^{21} Pa s. The $\dot{J}_4$ from *Nerem and Klosko* [1995] and the SLR analysis carried out in this section agree within 2σ, but the sign is opposite with respect to the model predictions. Our modelling, with a mantle viscosity of 10^{21} Pa s, agrees in amplitude and sign with *Cheng et al.* [1997] but only in amplitude with the SLR analysis by *Devoti et al.* [2001]. For $\dot{J}_6$, our SLR analysis agree with *Cheng et al.* [1997], and is coherent with our model predictions as far as the amplitude is concerned, but is opposite in sign. These findings show that discrepancies still exist between model predictions and the various SLR analyses, as well as among the SLR analyses themselves.

Trade-Off Between the Lower Mantle Viscosity and Present-Day Mass Imbalance in Antarctica and Greenland

In the previous section, comparison between SLR retrieved zonals and predictions from viscoelastic models driven solely by Pleistocenic deglaciation has shown that this mechanism cannot be the only source of time variations of the gravity field [*Devoti et al.*, 2001]. In fact, discrepancies in the viscosity profiles required to reproduce the different zonals when the only forcing mechanism is postglacial rebound seem to indicate ongoing mass redistribution over the Earth, related to global changes, eventually associated with mass instabilities in Antarctica and Greenland.

Both the even and odd zonal geopotential components of the gravity field, up to harmonic degree $l = 6$, are used in this section in conjunction with the modelled ones to enlighten the potential effects of ice mass imbalance in Antarctica and Greenland, which are thought to be the possible contributors to ongoing mass redistribution, on the inferences of the lower mantle viscosity.

The $\dot{J}_{odd}$ contribution of *Devoti et al.* [2001] can be better estimated by the following expression appropriate for a single satellite solution (Starlette) [*Schutz et al.*, 1993] instead of assuming $\dot{J}_{odd} = \dot{J}_3 + 0.9\dot{J}_5$ as in Table 2

$$\begin{aligned} \dot{J}_{odd} &= \dot{J}_3 + 1.04\dot{J}_5 - 0.53J_7 - 0.81\dot{J}_9 + 0.13\dot{J}_{11} \\ &\quad +0.52\dot{J}_{13} + 0.06\dot{J}_{15} - 0.3\dot{J}_{17} - 0.11\dot{J}_{19} + 0.14\dot{J}_{21} \end{aligned} \tag{2}$$

The highest odd zonals are not considered, since they would enter equation (2) with coefficients smaller than 0.1.

In the following Figure 3, we assume ice loss in Antarctica of -500 Gt/yr, corresponding to the upper bound of the range of -500 to $+400$ Gt/yr, as allowed by previous observations of grounded ice [*Bentley and Giovinetto*, 1991; *Jacobs*, 1992; *Warrick et al.*, 1996]. For Greenland we consider the case of ice loss of -144 Gt/yr, corresponding to a sea-level rise of 0.4 mm/yr for a 1 ^{o}C warming [*Oerlemans*, 1991]. The viscoelastic part of the Earth model is only needed for the Pleistocenic deglaciation, while present day mass imbalance in Antarctica and Greenland

requires the elastic component. Figure 3 portrays the dependence of the $\dot{J}_l$ on the lower mantle viscosity and on the rate of melting in the polar regions. The $\dot{J}_l$ are shown as a function of lower mantle viscosity for Pleistocene (solid), Pleistocene plus ice loss in Antarctica of -500 Gt/yr (dashed), and Pleistocene plus ice loss in Antarctica and Greenland of -500 and -144 Gt/yr respectively (dotted), with $\dot{J}_{odd}$ based on the equation (2). We notice the sensitivity of the zonals to lower mantle viscosity variations and the dominant effect of ice loss in Antarctica with respect to Greenland. The peak value in the $\dot{J}_l$ in the solid curves for the Pleistocene deglaciation is displaced from 2×10^{22} Pa s, corresponding to $\dot{J}_2$, towards lower values of lower mantle viscosity for increasing harmonic order in agreement with *Mitrovica and Peltier* [1993], down to 3×10^{21} Pa s for $\dot{J}_6$. The modeled zonals show the tendency to admit two intersections of the model results with the horizontal stripes depicting the *Cheng et al.* [1997] and *Devoti et al.* [2001] zonal secular drifts, green and red respectively, thus providing two possible lower mantle viscosities. The lower viscosity solution corresponds to a situation of sustained flow in the mantle and a present day configuration which is close to global post-glacial isostatic equilibrium, while the higher viscosity solution corresponds to reduced mantle flow and large isostatic inequilibrium. The solid curves show that Pleistocenic forcing does not allow a simultaneous fit of the SLR data for all the zonals with the same lower mantle viscosity. The scenarios of ice mass imbalance in Antarctica and Greenland suggest that this inconsistency, already noted in *Devoti et al.* [2001] and in the previous section, could be due to some amount of ice mass instability occurring today in these two regions, not included in the solid curves. The dashed and dotted curves show how ice loss in Antarctica and Greenland impact the results of the Pleistocenic deglaciation. With respect to the Pleistocenic solid curves, the effects of melting in Antarctica is to displace the peak values in $\dot{J}_l$ in the direction of the *Cheng et al.* [1997] and *Devoti et al.* [2001] data for the even and odd zonals, eventually exceeding the data themselves as shown by the dashed curves for $\dot{J}_6$ and the odd zonals because of the extreme value of -500 Gt/yr used in the simulations. Comparison between the dashed and dotted curves shows that ice loss in Greenland reinforces the effects of Antarctica on the even zonals and counteracts Antarctica on the odd ones [*Mitrovica and Peltier*, 1993; *James and Ivins*, 1997]. These results indicate that ice growth in Antarctica must be excluded, because it would cause a displacement of the Pleistocene curves in the opposite direction with respect to *Cheng et al.* [1997] and *Devoti et al.* [2001] and at the same time they suggest that present day mass imbalance could allow to solve for the inconsistencies in the lower mantle viscosity inferences noted above.

Conclusions

These results show that the SLR low degree even and odd zonal drifts of the gravity field can be used to constrain the rheology of the mantle and lithospheric thickness. Discrepancies in the viscosity values necessary to fit the zonal rates when Pleistocenic deglaciation is the only forcing mechanism is a strong indication that mass redistribution is actually occurring over the Earth, eventually associated with mass instabilities in Greenland and Antarctica, as also suggested by *Johnston and Lambeck* [1999].

Acknowledgments. This work is supported by the GOCE-Italy project funded by the Italian Space Agency

Table 1. Even degree zonal secular drift estimated by different authors, units: 10^{-11} /year

Author	$\dot{J}_2$	$\dot{J}_4$	$\dot{J}_6$
Yoder et al. [1983]	-3		
Rubincam [1984]	-2.6 ± 0.6		
Cheng et al. [1989]	-2.5 ± 0.3	0.3 ± 0.6	
Gegout and Cazenave [1993]	-2.8 ± 0.4		
Eanes [1995]	-2.4 ± 0.2		
Nerem and Klosko[1995]	-2.8 ± 0.3	0.2 ± 1.5	
Cazenave et al. [1995]	-3.0 ± 0.5	-0.8 ± 1.5	
Cheng et al.[1997]	-2.7 ± 0.4	-1.4 ± 1.0	0.3 ± 0.7
Devoti et al. [2001]	-2.9 ± 0.2	0.6 ± 0.5	0.3 ± 0.3

Table 2. Odd degree zonal secular drift estimated by different Authors, units: 10^{-11} /year

Author	$\dot{J}_3$	$\dot{J}_5$	$\dot{J}_{odd}$ $(\dot{J}_3 + 0.837\dot{J}_5)$	$\dot{J}_{odd}$ $(\dot{J}_3 + 0.9\dot{J}_5)$
Nerem and Klosko [1995]			1.6 ± 0.4	
Cheng et al. [1997]	-1.3 ± 0.5	2.1 ± 0.6	0.5	0.6
Devoti et al. [2001]				0.5 ± 0.2

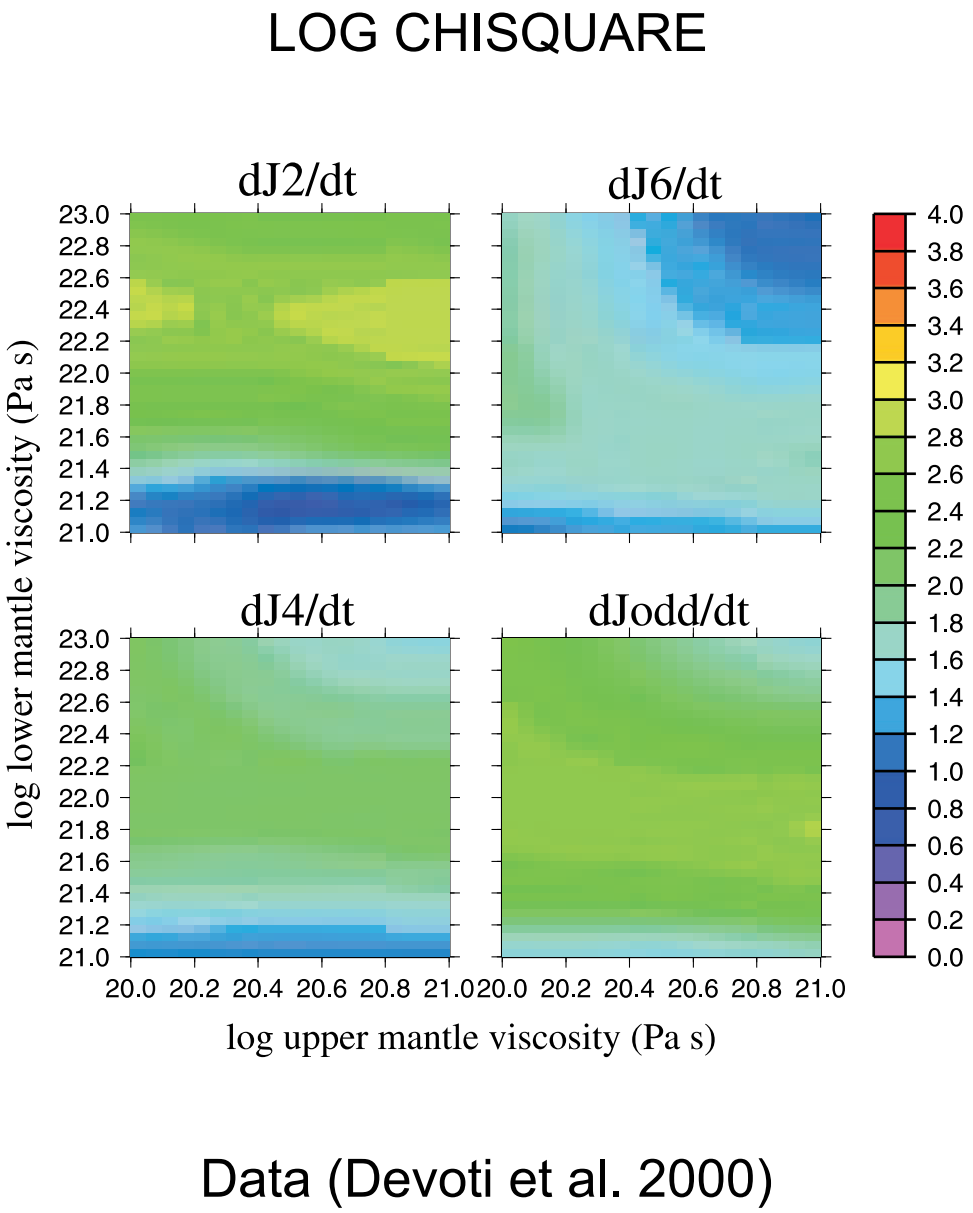

Figure 1. Logarithm of χ^2 plotted as a function of the logarithm of upper and lower mantle viscosity for $\dot{J}_2$, $\dot{J}_4$, $\dot{J}_6$ and $\dot{J}_{odd}$

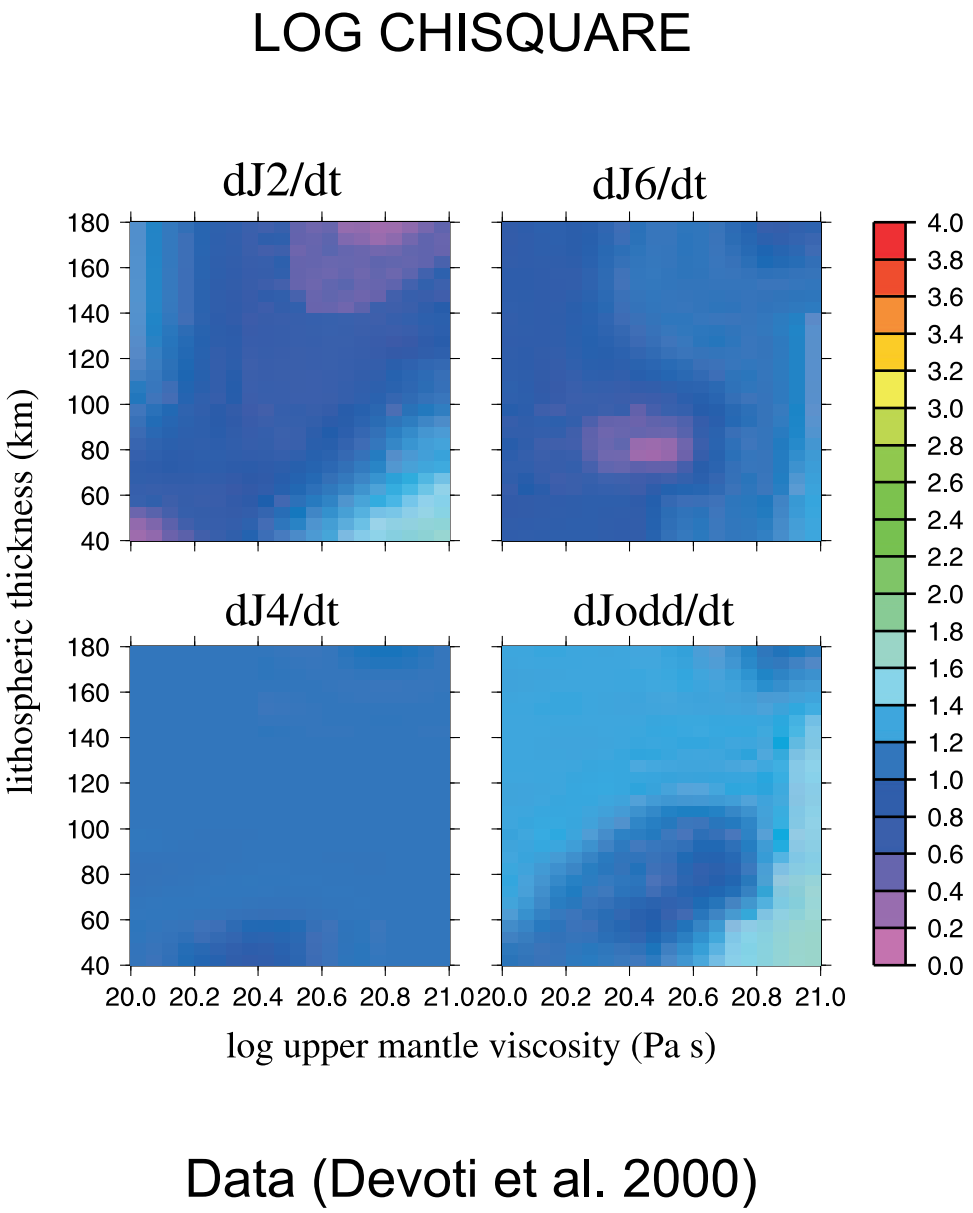

Figure 2. Logarithm of χ^2 plotted as a function of the logarithm of the lower mantle viscosity and lithospheric thickness for $\dot{J}_2$, $\dot{J}_4$, $\dot{J}_6$ and $\dot{J}_{odd}$

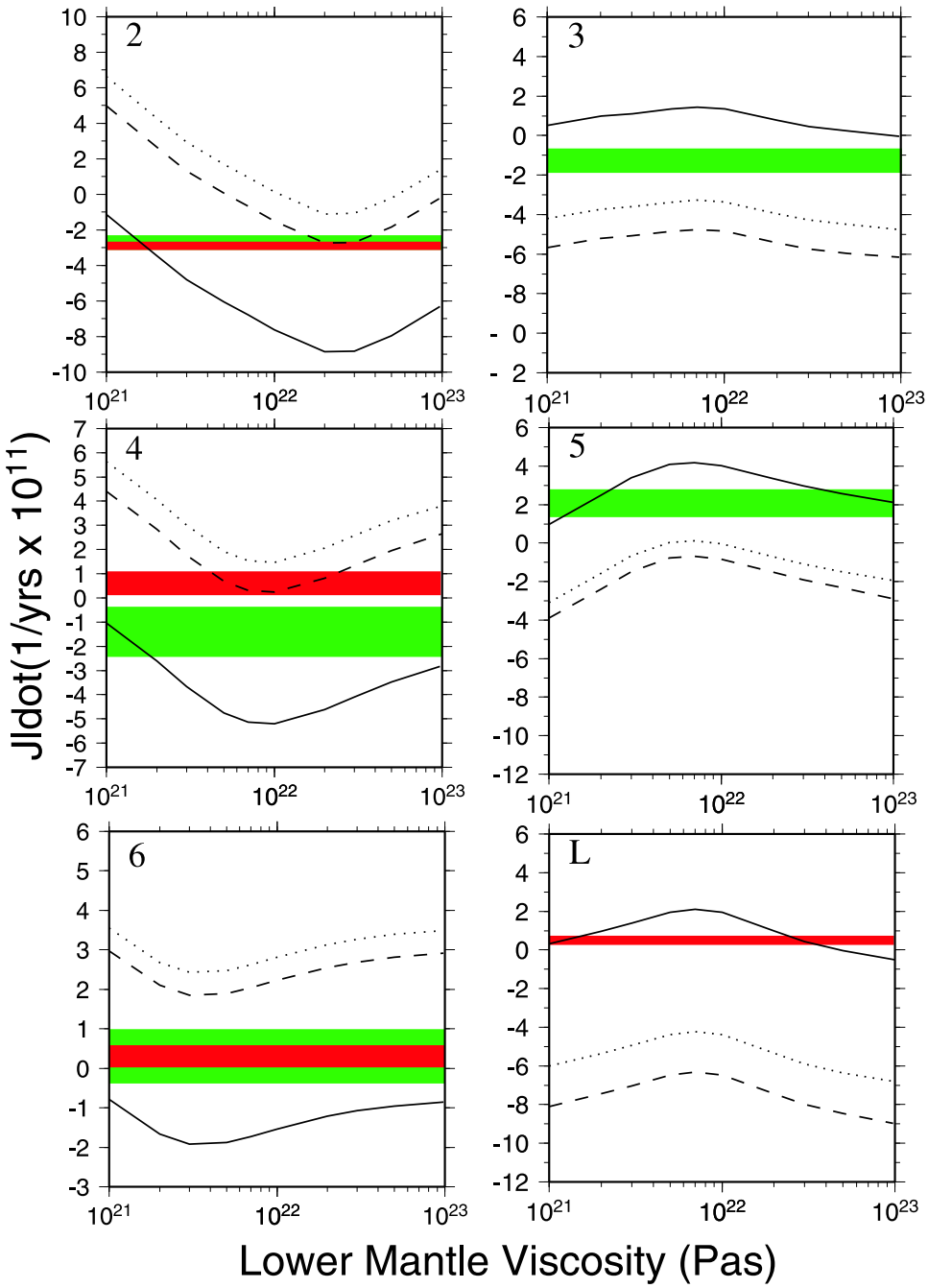

Figure 3. $\dot{J}_l$ as a function of lower mantle viscosity, ranging from 10^{21} 10^{23} Pa s. Upper mantle viscosity is fixed at 5×10^{20} Pa s. The green and red stripes stand for the *Cheng et al.* [1997] and *Devoti et al.* [2001] solutions. Solid curves correspond to Pleistocene deglaciation, dashed ones to Pleistocene plus maximum ice loss in Antarctica and the dotted ones include maximum ice loss in Greenland. The modeled results for $\dot{J}_{odd}$ stand for the combination of zonals given by equation (1).

References

Bentley, C.R. and M.B. Giovinetto, Mass balance of Antarctica and sea level change *In:* Weller, G., C.L. Wilson and B.A. Severin, *eds International Conference on the Role of Polar Regions in Global Change, University of Alaska, Fairbanks, AK, Vol. II.* 481-488, 1991.

Cazenave, A.A., P Gegout, G. Ferhat and P. Biancale, Temporal variations of the gravity field from LAgeos 1 and Lageos 2, in *Global Gravity and Its temporal Variations, IAG Symp., 116*, edited by R.H. Rapp, A.A. Cazenave and R.S. Nerem, Boulder, 1995.

Cheng, M.K., R.J. Eanes, C.K. Shum, B.E. Shutz and B. Tapley, Temporal variations in low-degree zonal harmonics from Starlette orbit analysis, *Geophys. Res. Lett.*, **16**, 393-396, 1989.

Cheng, M.K., C.K. Shum, and B.D. Tapley, Determination of long-term changes in the Earth's gravity field from satellite laser ranging observations, *J. Geophys. Res.*, **102**, 22,377-22,390, 1997.

Devoti, V. Luceri, C. Sciarretta, G. Bianco, G. Di Donato, L. L. A. Vermeersen, and R. Sabadini, The SLR secular gravity variations and their impact on the inference of mantle rheology and lithospheric thickness, *Geophys. Res. Lett.*, **28**, , 855-858, 2001.

Eanes, R.J., A study of temporal variations in Earth's gravitational field using Lageos 1 laser range observations, *CSR Report 95-8*, University of Texas, Austin, 1995.

Forte, A.M. and J.X. Mitrovica, New inferences of mantle viscosity from joint inversion of long-wavelength mantle convection and post-glacial rebound data, *Geophys. Res. Lett.*, **23**, 1147-1150, 1996.

Gegout, P. and A. Cazenave, Temporal variations of the Earth's gravity field for 1985-1989 from Lageos, *Geophys. I. Int.*, **114**, 347-359, 1993.

Jacobs, S., Is the Antarctic ice sheet growing?, *Nature*, **360**, 29-33, 1992.

James, T.S. and E.R. Ivins, Global geodetic signatures of the Antarctic ice sheet, *J. Geophys. Res.*, **102**, 605-633, 1997.

Johnston, P. and K. Lambeck, Postglacial rebound and sea level contributions to changes in the geoid and the Earth's rotation axis, *Geophys. J. Int.*, **136**, 537-558, 1999.

Mitrovica, J.X., and W.R. Peltier, Present-day secular variations in the zonal harmonics of earth's geopotential, *J. Geophys. Res.*, **98,** 4,509-4,526, 1993.

Nakada, M. and K. Lambeck, Late Pleistocene and Holocene sea level change in the Australian region and mantle rheology, *Geophys. J. Int.*, **96**, 497-517, 1989.

Nerem, R.S. and S.M. Klosko, Secular variations of the zonal harmonics and polar motions as geophysical constraints, *In:* Global Gravity Field and Its Temporal Variations, *eds* R.H. Rapp , A. Cazenave, R.S. Nerem, 152-163, Springer-Verlag, New York, 1996.

Oerlemans, J., The mass balance of the Greenland ice sheet: sensitivity to climate change as revealed by energy balance modelling, *The Holocene*, **1**, 40-49, 1991.

Rubincam, D.P., Postglacial rebound observed by LAGEOS and the effective viscosity of the lower mantle, *J. Geophys. Res.*, **89**, 1077-1087, 1984.

Schutz, B.E., M.K. Cheng, R.J. Eanes, C.K. Shum and B.D. Tapley, Geodynamic results from Starlette orbit analysis, *In*: Contributions of space geodesy to geodynamics: earth dynamics, *eds:* Smith D.E., D.L., Turcotte, Geodynamics Series, AGU, Washington DC, **24**, 175, 1993.

Tushingham, A.M., and W.R. Peltier, ICE-3G: A new global model of late Pleistocene deglaciation based upon geophysical predications of postglacial relative sea level change, *J. Geophys. Res.*, **96**, 4,497-4,523, 1991.

L. L. A. Vermeersen, and R. Sabadini, Devoti, V. Luceri, P. Rutigliano, C. Sciarretta and G. Bianco, Mantle viscosity inferences from joint inversion of Pleistocene deglaciation-induced chenges in geopotential with new SLR analysis and polar wander, *Geophys. Res. Lett.*, **25**, 4261-4264, 1998.

Warrick, R.A., C. le Provost, M.F. Meier, J. Oerlemans and P.L. Woodworth, Changes in sea level. *In*: Houghton, J.T., L.G. Meira Filho, B.A. Callander, N. Harris, A. Kattenberg and K. Maskell, *eds. Climate Change 1995: the science of climate change* Cambridge Univ. Press, Cambridge, 359-405, 1996.

Yoder, C.F., J.G. Williams, J.O. Dickey, B.E. Shutz, R.J. Eanes, and B.D. Tapley, Secular variations of earth's gravitational harmonc J_2 coefficient from Lageos and nontidal acceleration of Earth rotation, *Nature*, **303**, 757-762, 1983.